



# Neuroimaging Findings in COVID-19 Associated Rhino-Orbital-Cerebral Mucormycosis: A Review

Anjuna Reghunath<sup>1</sup>  Rohini Gupta Ghasi<sup>1</sup> Anuradha Sharma<sup>1</sup> Neha Bagri<sup>1</sup> Swarna Gupta Jain<sup>1</sup>

<sup>1</sup>Department of Radiodiagnosis, Vardhman Mahavir Medical College and Safdarjung Hospital, New Delhi, India

Address for correspondence Rohini Gupta Ghasi, MD, Department of Radiodiagnosis, Vardhman Mahavir Medical College and Safdarjung Hospital, New Delhi-110029, India (e-mail: rohini1912@gmail.com).

Indian J Radiol Imaging 2022;32:224–234.

## Abstract

The involvement of the neurological system by coronavirus has been well established. Since its onset, the systemic manifestations of coronavirus disease 2019 (COVID-19) have been evolving rapidly and imaging plays a pivotal role in diagnosing the various primary and secondary effects of the disease. As the pandemic continues to defy human civilization, secondary impacts of the disease and the treatment given to patients afflicted with the disease have stemmed up. Rhino-orbital-cerebral mucormycosis is one such potentially dangerous infection now commonly seen in COVID-19 patients, especially the ones treated with immunosuppressants. Early diagnosis is key for COVID-19-associated mucormycosis (CAM), and radiologists should be well aware of its alarming neurological manifestations from the involvement of parenchyma, meninges, vessels, cranial nerves, and skull base. This review highlights the magnetic resonance imaging features of neuraxial involvement in CAM.

## Keywords

- ▶ magnetic resonance imaging
- ▶ computed tomography
- ▶ mucormycosis
- ▶ COVID-19
- ▶ ROCM
- ▶ neuroimaging

## Introduction

The coronavirus disease 2019 (COVID-19) pandemic continues to have an enormous impact on the population of the world. Rhino-orbital-cerebral mucormycosis (ROCM) is a potentially fatal angioinvasive secondary fungal infection which has shown a growing trend during the COVID-19 pandemic, currently referred to as COVID-19-associated mucormycosis (CAM).<sup>1,2</sup> In all anatomical sites, tissue invasion and angioinvasion are the trademarks of mucormycosis.<sup>3,4</sup> Central nervous system (CNS) affliction represents one of the most morbid manifestations of mucormycosis and often governs the survival and functional outcome of the patient.<sup>4</sup> Prior to the pandemic, ROCM had a reported incidence of 0.005 to 1.7/million, which has massively increased since 2021.<sup>2</sup> The main risk factors found for CAM were diabetes and steroid use.<sup>2</sup> Compared with non-COVID ROCM, patients most affected with CAM were middle-

aged, diabetic males with recent COVID-19 infection. New-onset upper jaw toothache and loosening of teeth were striking symptoms and neurological manifestations, such as headache, proptosis, vision loss, extraocular movement restriction, cavernous sinus, meningeal, and parenchymal involvement were common in CAM. Also, stroke in CAM was found to follow a definitive pattern with watershed infarction.<sup>3</sup> An aggressive diagnostic approach and timely initiation of antifungal therapy are imperative to reduce morbidity and mortality.<sup>5</sup>

## Pathophysiology

A multitude of factors, including pre-existing diseases, such as diabetes mellitus, previous respiratory compromise, use of immunosuppressive therapy and steroids, and systemic immune alterations of COVID-19 infection have been suggested in the etiopathogenesis of this recent surge in cases.<sup>6</sup> A

published online  
July 13, 2022

DOI <https://doi.org/10.1055/s-0042-1750158>.  
ISSN 0971-3026.

© 2022. Indian Radiological Association. All rights reserved.

This is an open access article published by Thieme under the terms of the Creative Commons Attribution-NonDerivative-NonCommercial-License, permitting copying and reproduction so long as the original work is given appropriate credit. Contents may not be used for commercial purposes, or adapted, remixed, transformed or built upon. (<https://creativecommons.org/licenses/by-nc-nd/4.0/>)

Thieme Medical and Scientific Publishers Pvt. Ltd., A-12, 2nd Floor, Sector 2, Noida-201301 UP, India

propensity of the virus to cause widespread lung involvement is found to raise the risk of invasive fungal infections.<sup>6</sup> Another proposed mechanism is the alteration in innate immunity secondary to immune dysregulation seen in COVID-19, with reduced numbers of T lymphocytes, CD4 + T, and CD8 + T cells.<sup>6</sup>

Fungi of the genus *Rhizopus* account for the majority of the cases, followed by *Lichtheimia* (formerly known as *Absidia* and *Mycocladius*), and *Mucor*.<sup>7</sup> Overall, *Rhizopus oryzae* is the most prevalent pathogen isolated from specimens.<sup>7</sup> The larger aseptate hyphae of Mucorales impede entry to the meningeal microcirculation causing a more localized disease leading to cerebritis, abscess formation, or involvement of larger vessels. The immune status and inflammatory response of the host determine the degree of CNS involvement.<sup>5</sup>

### Clinical Course of Rhino-Orbital-Cerebral Mucormycosis

In the head and neck location, mucor infection can be divided into isolated nasal, rhino-orbital, or ROCM.<sup>8</sup> In the appropriate clinical settings, invasive fungal sinusitis is clinically detected as a painless, necrotic ulcer (eschar) in the nasal septum and sinusitis, followed by bony erosion and spread into adjacent structures like palate, orbit, and brain, with a fulminant progression over a few days to weeks, usually leading to death.<sup>9</sup> Symptoms include fever, nasal congestion or discharge, facial pain or numbness, and epistaxis. Intra-orbital extension leads to proptosis and visual disturbances, while intracranial spread results in headache, mental status changes, seizures, neurological deficits, and coma.<sup>9</sup> Definitive diagnosis is by nasal biopsy and culture, which reveals

broad aseptate filamentous fungal hyphae.<sup>6</sup> Liposomal amphotericin B with sinus debridement using an endoscopic approach for early disease and open surgery and exenteration for extensive disease is the preferred management regime for ROCM.<sup>4</sup> Neurosurgical intervention is directed in raised intracranial pressure (e.g., hemispheric stroke), obstructive hydrocephalus, and for lesions, compressing the spinal cord.<sup>4</sup>

### Mechanism of Spread

Four main mechanisms proposed for the spread of ROCM are direct, perineural, perivascular, and hematogenous spread (– Fig. 1). The clinical manifestations and involved sites in each individual depend on the mode(s) of spread and the extent of involvement by the disease process.<sup>10</sup>

**1. Direct infiltration:** Involvement of the CNS occurs most frequently (70%) due to contiguous spread from the paranasal sinuses and orbits.<sup>4</sup> The disease process initially spreads via the dehiscent lamina papyracea, anterior and posterior ethmoid orifices, involving the orbit, pterygopalatine fossa, periantral fat, nasolacrimal duct, lacrimal sac, and rarely the nasopharynx.<sup>11</sup> Direct infiltration into frontal lobes (gyrus recti) may occur through the cribriform plate or from frontal sinus,<sup>10</sup> while the extension to middle cranial fossa occurs through cavernous sinus.<sup>3</sup>

**2. Perineural spread:** Emerging studies have demonstrated the possible perineural spread of infection both microscopically and macroscopically.<sup>10</sup> Sravani et al found perineural spread on biopsy specimens in 50% cases in a study of 30 patients afflicted by ROCM, even for a substantial distance from the primary focus of infection.<sup>12</sup> Direct spread

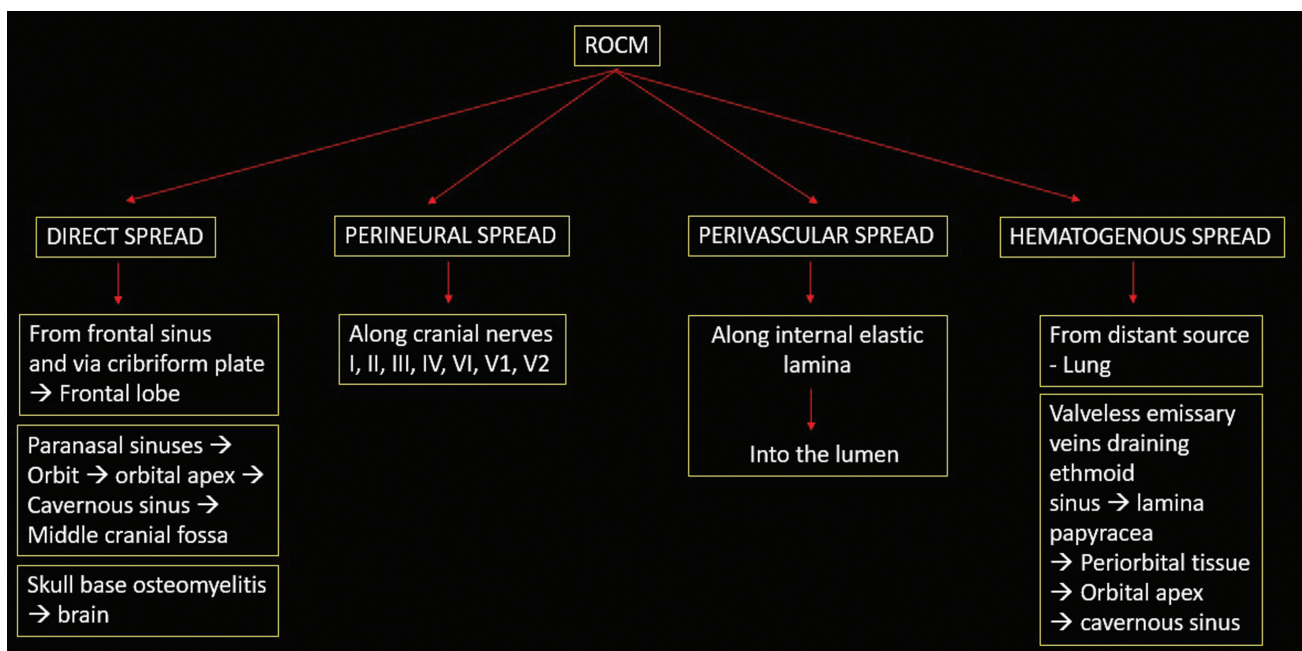


**Fig. 1** Methods of neuraxial spread of rhino-orbital-cerebral mucormycosis (ROCM).

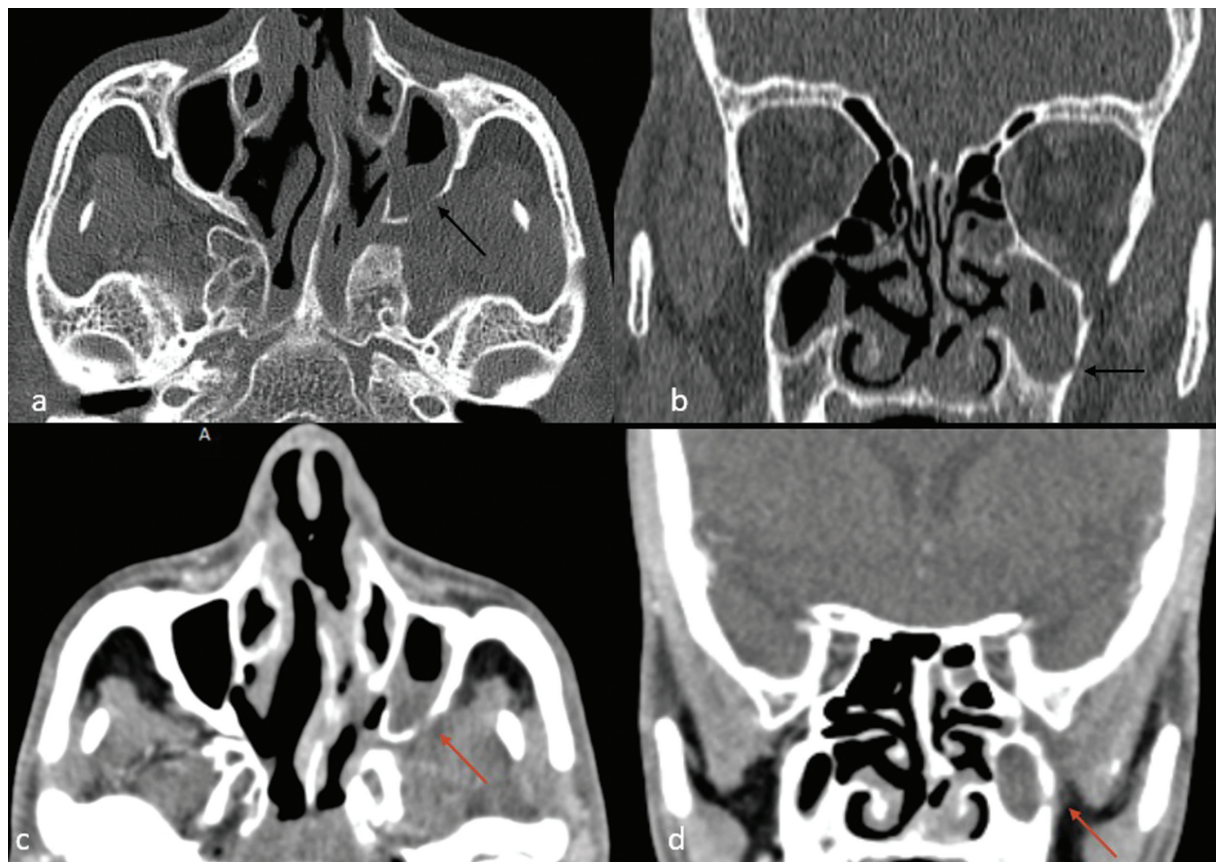


**Fig. 2** NCCT of paranasal sinuses in a 35-year-old male COVID-19 patient with sinonasal mucormycosis shows bilateral maxillary and left ethmoid sinusitis with subtle erosion of the posterolateral wall of the left maxillary sinus (black arrow) on axial (a) and coronal reformat (b) images in bone window, along with periantral fat obliteration with soft tissue (red arrow) on corresponding soft tissue window images respectively (c, d). COVID-19, coronavirus disease 2019; NCCT, noncontrast computed tomography.

through the cribriform plate into the anterior cranial fossa has been suggested to represent perineural spread via olfactory nerves by some authors.<sup>12</sup> Galletta et al demonstrated V1 trigeminal branch division infiltration in a patient with invasive mucormycosis.<sup>10</sup> V2 trigeminal root involvement, retrogradely via the infraorbital nerve to middle cranial fossa through the inferior orbital fissure and foramen rotundum, and involvement of intracisternal tract of the trigeminal nerve and Meckel's cave have also been reported.<sup>10</sup>

**3. Perivascular spread:** Vascular tropism is the hallmark of mucor infection. Fungal spores tend to invade vessels and strongly adhere to endothelial cells. Also, *R. oryzae* produces an alkaline protease that cleaves elastin and separates the internal elastic lamina from the media. Fungal hyphae extend along the internal elastic lamina and further into the arterial lumen, obliterating it with intimal hyperplasia and thrombosis and, thus, leading to infarction, vasculitis, and necrosis of involved tissues.<sup>10</sup>

**4. Hematogenous dissemination:** This may occur from a distant focus like the lung with predilection for gray-white matter junction or via the valveless emissary veins draining the ethmoid sinus, traversing the lamina papyracea, and facilitating fungal infiltration of periorbital tissue, the orbital apex, and the cavernous sinus.<sup>10</sup>

## Imaging of Rhino-Orbital-Cerebral Mucormycosis

Imaging plays a very important role in diagnosing and evaluating the extent of this serious condition. Computed tomography depicts hypoattenuating mucosal thickening of paranasal sinuses, and a tendency to involve ethmoid and sphenoid sinuses unilaterally has been reported.<sup>9</sup> Bone erosion may be very subtle and suggested by obliteration of periantral fat (→ Fig. 2). Significant bony destruction of the sinus walls may occur rapidly with intraorbital and intracranial extension of the inflammation.<sup>9</sup> On magnetic resonance (MR) imaging, the compacted fungal hyphae present low signal intensity on T2-weighted sequences due to the presence of paramagnetic substances and associated tissue necrosis from mucosal angioinvasion.<sup>10</sup> The “black turbinate sign” refers to nonenhancing portions in the turbinate on T1-weighted post-contrast images owing to infarction from angioinvasion of the fungus (→ Fig. 3).<sup>13</sup>

Intraorbital invasion is suggested by thickening and lateral displacement of the medial rectus muscle, orbital fat infiltration, preseptal or postseptal cellulitis, endophthalmitis, and subperiosteal or intraorbital abscess. When proptosis from orbital cellulitis is significant, the dorsal globe becomes



**Fig. 3** MRI of sinonasal region done in a 42-year-old COVID-19 patient with culture proven mucormycosis reveals non-enhancing areas within the left inferior turbinate (black arrow) on T1W fat saturated postcontrast axial (a) and coronal (b) images, suggestive of “black turbinate sign.” COVID-19, coronavirus disease 2019; MRI, magnetic resonance imaging.

deformed, with tenting of its posterior aspect, and depicts the “guitar pick” sign (►Fig. 4).<sup>14</sup> Orbital apex syndrome is a morbid manifestation, which leads to complete ophthalmoplegia and rapid vision loss, due to the involvement of cranial nerves II, III, IV, V, and VI.<sup>6</sup> Restricted diffusion may be the earliest detectable abnormality in acute ischemic optic neuropathy due to rhinocerebral mucormycosis.<sup>15</sup>

### Neurological Manifestations

1. **Cavernous sinus involvement**—The cavernous sinus is often the first intracranial structure to be involved. Intracra-

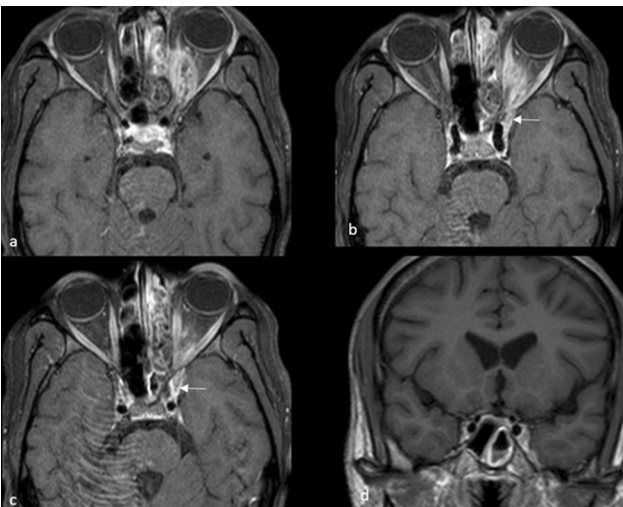


**Fig. 5** MRI brain imaging done in a 22-year-old COVID-19 patient with culture-proven mucormycosis demonstrates bilateral ethmoid sinusitis and contiguous left orbital spread of disease on axial T1W fat suppressed postcontrast images (a, b). A focal non-enhancing region is seen in the left cavernous sinus (white arrow), causing mild lateral bulging of the wall of left cavernous sinus on axial (c) and coronal (d) contrast-enhanced images, suggesting cavernous sinus thrombosis. Flow void of cavernous segment of left internal carotid artery is maintained and normal in caliber. Note is made of sphenoid sinusitis as well. COVID-19, coronavirus disease 2019; MRI, magnetic resonance imaging.

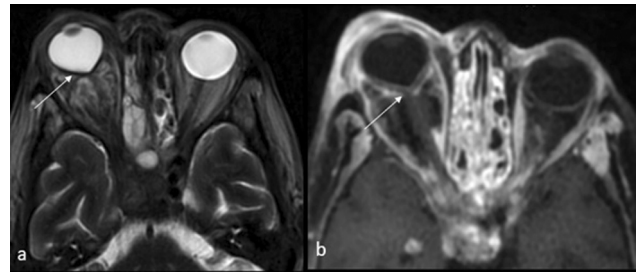


**Fig. 4** MRI of orbits in another 52-year old patient with similar history depicts right proptosis and deformity of posterior globe or “guitar pick sign” (white arrow) secondary to right orbital compartment syndrome on axial T2W fat saturated (a) and T1W fat saturated postcontrast (b) images. MRI, magnetic resonance imaging.

nial extension of disease through sphenoid sinus or orbital apex often leads to cavernous sinus thrombosis as evidenced by bulging walls of the sinus with nonenhancing internal areas (►Fig. 5). There can be associated carotid artery invasion/occlusion leading to brain infarction or pseudoaneurysm formation with impairment of the function of cranial nerves III, IV, VI, and trigeminal nerve branches V1 and V2 that traverse it.<sup>9</sup>

2. **Infarcts**—Strokes in CAM are primarily due to cavernous internal carotid artery (ICA) involvement from intraluminal thrombosis, microscopic angioinvasion, vasospasm, or external compression.<sup>3</sup> The infarcts are majorly at external and internal watershed territories (►Fig. 6) of anterior cerebral artery and middle cerebral artery (MCA) or MCA and posterior cerebral artery, with or without hemorrhagic transformation.<sup>3</sup>

3. **Fungal meningitis**—Leptomeningeal enhancement due to fungal meningitis may be smooth or thick, nodular and irregular, long and continuous, poorly demarcated or asymmetric (►Fig. 7).<sup>5</sup> Enhancement (characteristically focal) of anterior and medial temporal poles was most common followed by frontal lobes in a study.<sup>3</sup>

4. **Intracranial granulomas**—Granulomas consist of lymphocytes, plasma cells, and fungal hyphae. Intracranial granulomas are typically hypointense on T1- and T2-weighted images with minimal postcontrast enhancement and mild perilesional edema (►Fig. 8).<sup>9</sup>

5. **Cerebritis**—On T1WI, fungal cerebritis appears as an iso- or hypointense area involving gray matter with subtle mass effect and minimal to no enhancement (►Fig. 9).<sup>5</sup> On T2WI and fluid-attenuated inversion recovery, they appear as hyperintense lesion, with areas of decreased signal intensity within the lesion due to the paramagnetic effects of metal ions.<sup>5</sup> These lesions usually present with restricted diffusion on diffusion-weighted imaging (DWI).<sup>5</sup>

6. **Brain abscess**—Fungal abscesses tend to be numerous and can involve the deep gray matter and basal ganglia.<sup>5</sup> On DWI, fungal abscesses demonstrate restricted diffusion in the abscess wall and intracavitary projections, with central core sparing (►Fig. 10).<sup>5</sup> On MR, the core appears hypointense on T1W and hyperintense on T2W images, with a surrounding isomildly hyperintense rim on T1WI, which

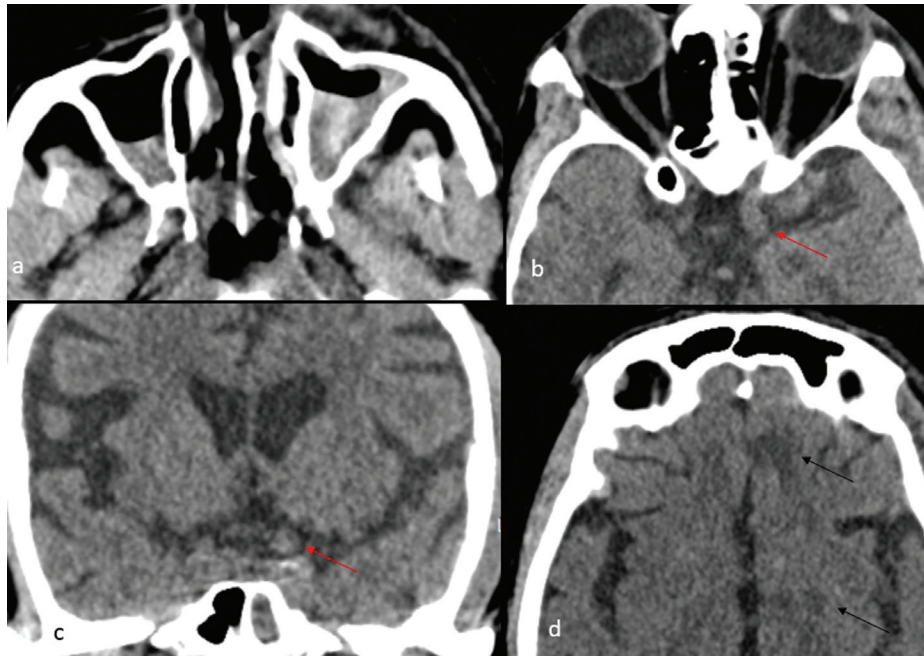


**Fig. 6** NCCT of brain of a 42-year-old COVID-19 recovered gentleman with left hemiparesis shows bilateral maxillary sinusitis with hyperdense internal contents on axial image (a), which was culture proven to be mucormycosis. There is subtle asymmetric fusiform enlargement of left cavernous internal carotid artery (red arrow) as compared with right side as seen on axial (b) and coronal reformat (c) images, suggesting mycotic aneurysm. Acute lacunar infarcts are also seen in left gyrus rectus and left globus pallidus (black arrows) (d). COVID-19, coronavirus disease 2019; NCCT, noncontrast computed tomography.

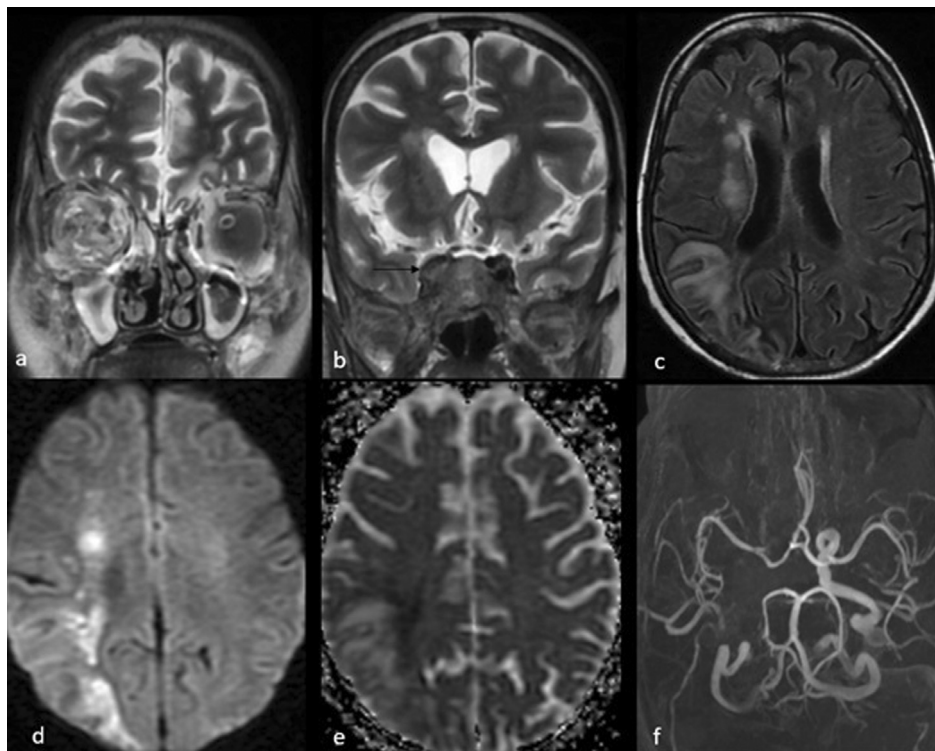


**Fig. 7** MRI of brain in a 52-year-old patient with rhino-orbital cerebral mucormycosis post-COVID-19 infection presented with left hemiparesis. T2W coronal images (a, b) demonstrate bilateral maxillary and ethmoid sinusitis with right orbital involvement and right cavernous sinus thrombosis with loss of flow void of cavernous and clinoid segments of right internal carotid artery (ICA) (black arrow). Axial FLAIR image (c) depicts hyperintense areas in right internal and external watershed territories, which appear hyperintense on diffusion weighted image (d) with corresponding hypointensity on ADC map (e), suggesting acute-early subacute infarct. Maximum intensity projection TOF (time-of-flight) MR angiography image shows non-visualization of intracranial part of right ICA, consistent with thrombosis. COVID-19, coronavirus disease 2019; FLAIR, fluid-attenuated inversion recovery; MRI, magnetic resonance imaging.

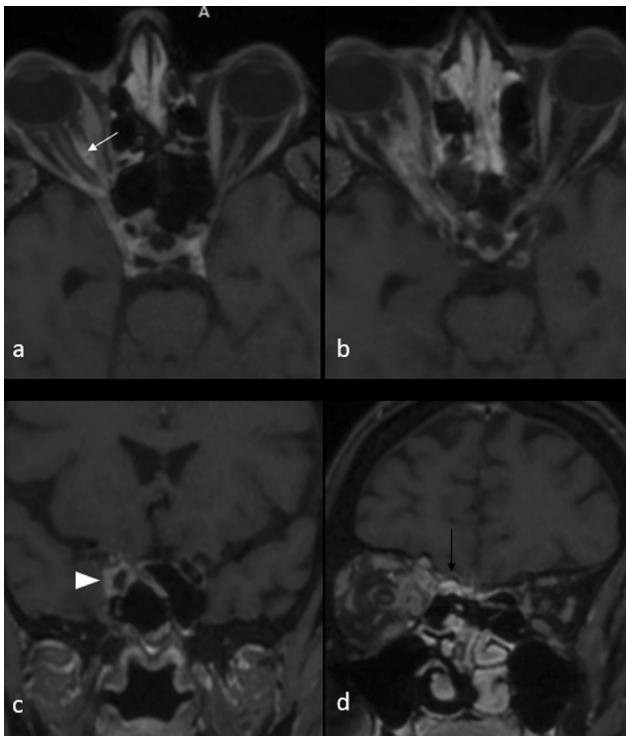


**Fig. 8** A 47-year-old COVID-19 in-patient treated with intravenous steroids developed nasal discharge and sudden right-sided loss of vision. Postcontrast T1W fat saturated axial (a, b) images reveal mild bilateral ethmoid sinusitis and right optic neuritis as suggested by bulky, enhancing right optic nerve with perineural enhancement (white arrow). The inflammation is extending along right optic nerve into the optic canal and orbital apex. Coronal T1W fat saturated postcontrast images (c, d) show further extension of infection to the right cavernous sinus, causing perivascular enhancement around right internal carotid artery (arrowhead). There is focal leptomenigitis in the right frontal lobe (black arrow) and involvement of right medial rectus and superior oblique muscle due to focal erosion of the cribriform plate and lamina papyracea respectively. Culture from sinonasal contents revealed mucormycosis. COVID-19, coronavirus disease 2019.

appears hypointense on T2WI. Peripheral enhancement is seen on T1W postcontrast enhancement sequence. Fungal abscesses may demonstrate lipids (1.2–1.3 ppm), lactate (1.3 ppm), alanine (1.5 ppm), acetate (1.9 ppm), succinate (2.4 ppm), and choline (3.2 ppm) on MR spectroscopy. A distinctive feature of fungal infections is the presence of disaccharide trehalose (3.6 ppm) in the abscess wall (► Fig. 10).<sup>5</sup>

**7. Obstructive hydrocephalus**—This may occur due to meningeal and cisternal exudates or infiltration of the cisterns/ventricular lining (► Fig. 11).<sup>4</sup>

**8. Mycotic aneurysms**—The elastic laminae of the vessel wall may get disrupted causing focal dilatation of artery and development of mycotic aneurysms, which can rupture resulting in intracranial bleed (► Fig. 12). Mycotic aneurysms are commonly seen within the anterior circulation, affecting long portions of proximal segments of the large cerebral vessels such as anterior, middle, or posterior cerebral arteries.<sup>5</sup>

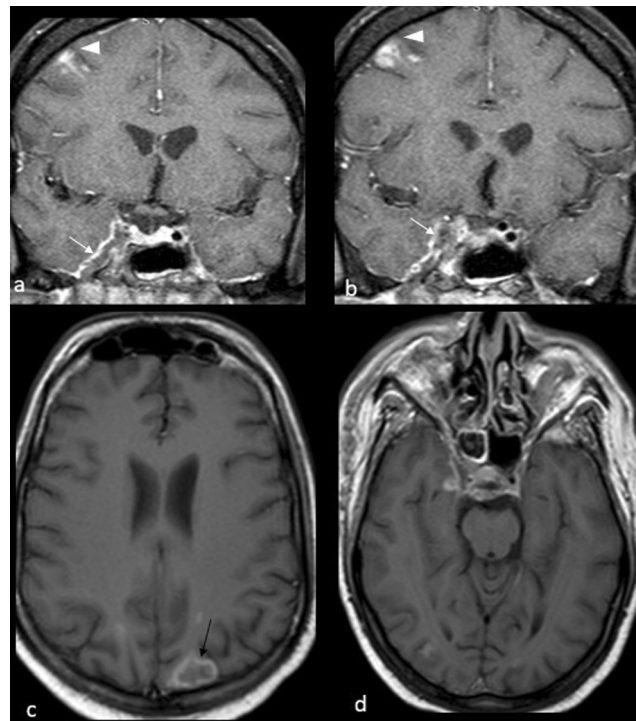


**Fig. 9** Coronal T1W postcontrast images (a, b) in a culture-proven case of invasive fungal sinusitis in a COVID-19 patient treated with antivirals and oral steroids demonstrate right cavernous sinus thrombosis (white arrow) with complete thrombosis of cavernous and clinoid segments of right internal carotid artery. Focal cerebritis is seen in the right frontal lobe (arrowhead). Conglomerated fungal granulomas showing peripheral enhancement is seen in left posterior parietal cerebral parenchyma (black arrow) and few tiny disk-enhancing fungal granulomas are also seen in bilateral parietal, temporo-occipital parenchyma and in right temporal lobe abutting right cavernous sinus on axial T1W postcontrast sequences (c, d). COVID-19, coronavirus disease 2019.

**9. Garcin syndrome**—It is the unilateral cranial nerve palsies without the involvement of sensory and motor tracts due to mycelial growth along the cranial nerves (► Fig. 13).<sup>16</sup>

**10. Skull base osteomyelitis**—Contiguous extension of pathology from the paranasal sinuses into the skull base is common and holds prognostic significance with involvement of pterygopalatine fossa, pterygoid wedge, vidian canal often requiring bone drilling (► Fig. 14).<sup>17,18</sup>

**11. Uncommon manifestations of cranial invasion** include sagittal sinus thrombosis, epidural, subdural, or suprasellar abscess (► Fig. 15).<sup>4</sup>

The imaging correlates along with the pathophysiology of various manifestations seen in neuraxial involvement by CAM are elaborated in ► Table 1.

## Conclusion

Patients with COVID-19 may develop a wide range of neurological symptoms, some of which may be attributed to CAM, which is now a well-established entity with the predominant risk factors being diabetes, immunodepletion, and steroid therapy in COVID-19 pneumonia.<sup>2</sup> Imaging helps in the early

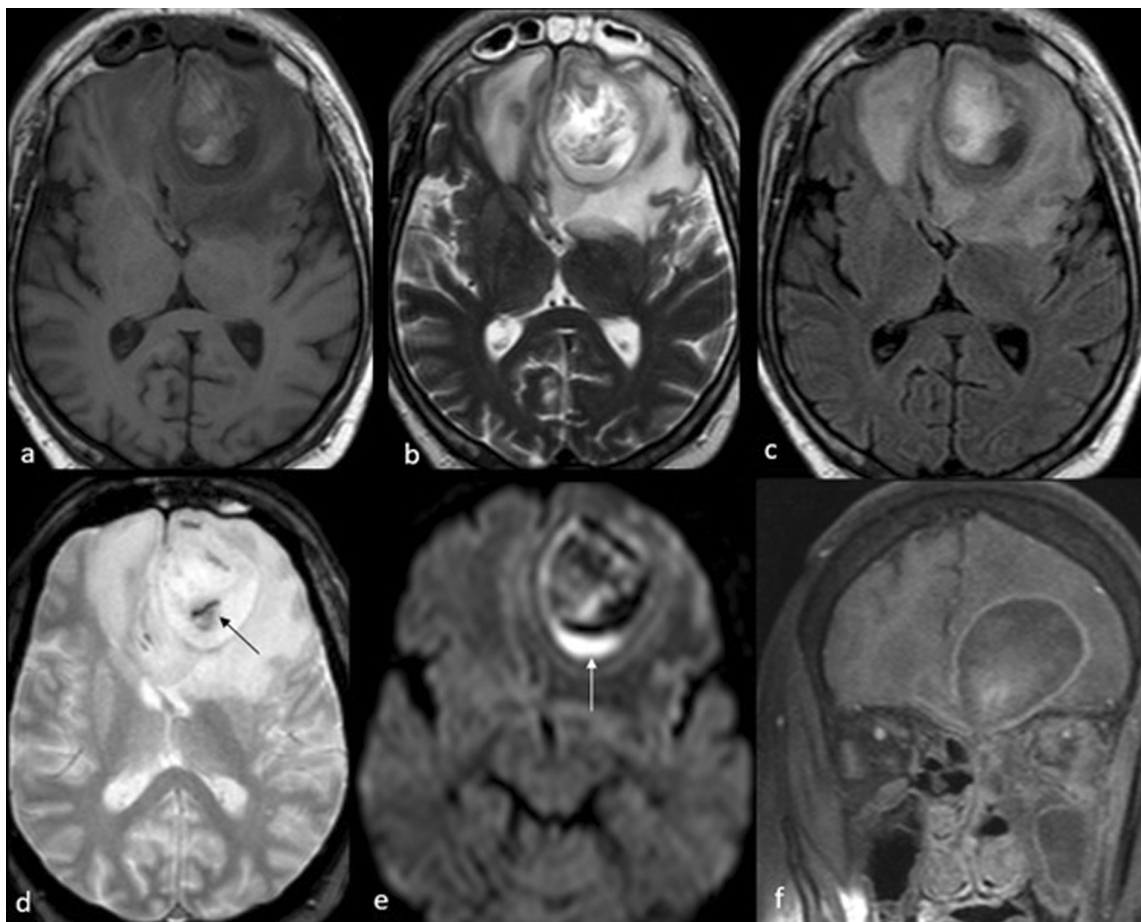


**Fig. 10** MRI brain in a 48-year-old patient with rhino-orbital-cerebral mucormycosis demonstrates a well-defined fungal abscess in left frontal parenchyma. On axial T1W image (a), the core of the lesion shows few hyperintense areas, while the wall appears hypointense to gray matter. T2W (b), FLAIR (c) images reveal heterogeneously hyperintense internal contents and T2W/ FLAIR hypointense wall. Note made of extensive perilesional edema, mild midline shift to right and effacement of frontal horns of bilateral lateral ventricles. Axial T2\* GRE image (d) shows focal internal blooming areas (black arrow), suggestive of bleed. There is diffusion restriction of wall of the abscess (white arrow) on axial DWI (e) and smooth rim enhancement on T1W fat saturated postcontrast coronal image (f). There is evidence of left maxillary and ethmoid invasive fungal sinusitis with involvement of left orbit. FLAIR, fluid-attenuated inversion recovery; GRE, gradient echo sequences; MR, magnetic resonance;

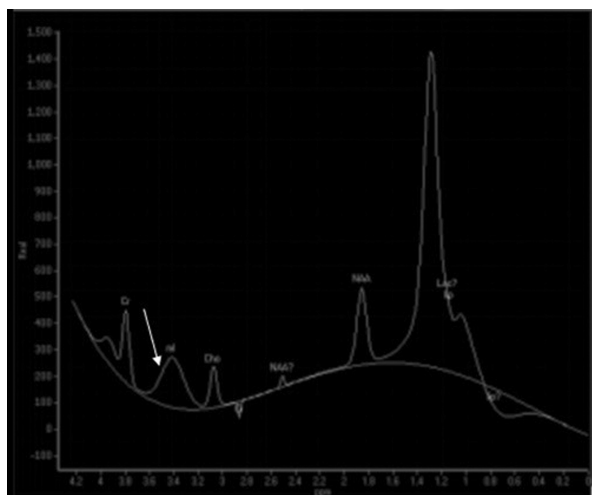


**Fig. 11** Single voxel proton MR spectroscopy was done by placing the ROI along the wall of the abscess in the same patient as in ► Fig. 10. Spectroscopy reveals a significant lipid-lactate peak at 1.2–1.3 ppm, small choline peak at 3.2 ppm and another peak at 3–4–3.6 ppm (white arrow), suggestive of substrate trehalose found in wall of fungal abscesses. MR, magnetic resonance; ROI, region of interest.

detection of neurological involvement of this serious condition, delineating the extent of intracranial infection and ruling out postsurgical residual disease (► Figs. 16 and 17). Due to the changing trends in the COVID-19 pandemic, it is an absolute necessity for all radiologists to have a high index of suspicion and be aware of the imaging features of ROCM and its possible complications, as prompt diagnosis and treatment with antifungal medication and surgical debridement can halt the progression of the infection. More effective prevention and treatment of severe COVID-19 infection through widespread vaccination, social distancing, and more efficacious antiviral therapy would positively decrease the incidence of CAM in the near future.<sup>2</sup>

#### Note

There are no prior publications or submissions with any overlapping information, including studies and patients. The work has not been presented elsewhere.

#### Funding

None.

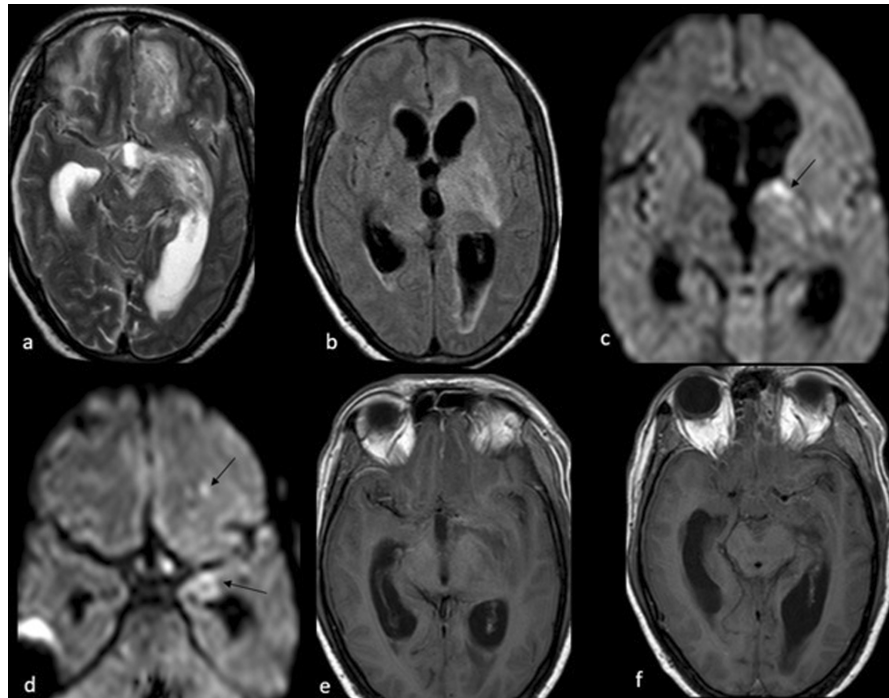


**Fig. 12** MRI in a 42-year-old COVID-19 patient who had developed culture-proven invasive sinonasal mucormycosis following a course of intravenous steroids are shown. T2W axial image (a) reveals heterogeneously hyperintense areas in suprasellar cistern, left parasagittal frontal cerebral region, and left medial temporal lobe, involving gray and white matter. Mild white matter edema is also seen in the right frontal lobe. T2W FLAIR axial image (b) shows hyperintensity in the adjoining left ganglio-capsulo-thalamic region with mild hydrocephalus and periventricular ooze. Diffusion weighted image (c, d) showed patchy diffusion restriction in the above-mentioned areas (black arrows). Postcontrast T1W axial images at the level of basal cisterns (e, f) reveal minimally enhancing exudates contiguously extending into the left basifrontal and temporal lobes, causing compression of anterior and left middle cerebral artery flow voids as well as extraventricular obstructive hydrocephalus. The diffusion restriction may be attributed to fungal cerebritis. COVID-19, coronavirus disease 2019; FLAIR, fluid-attenuated inversion recovery; MRI, magnetic resonance imaging.

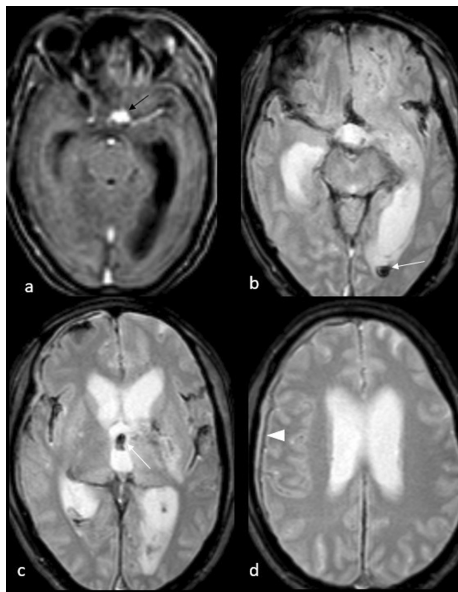


**Fig. 13** Contrast-enhanced MR angiography (a) in the same patient as in ► Fig 12 reveals mycotic aneurysm of the terminal part of left internal carotid artery (black arrow). Axial T2W gradient images (b–d) show low signal bleed lining bilateral Sylvian fissures, suprasellar cistern, right fronto-parieto-temporal dura, with a thin subdural hematoma in the fronto-parietal region (arrowhead). Note the bleed in occipital horn of left lateral ventricle and third ventricle (white arrow). Features are consistent with rupture of mycotic aneurysm with subarachnoid hemorrhage, intraventricular hemorrhage, and subdural hematoma. MR, magnetic resonance.

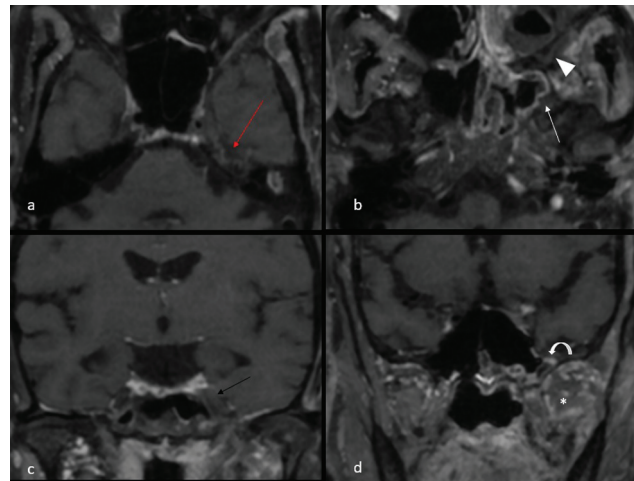


**Fig. 14** 3-D contrast enhanced MR scan in a 50-year-old male with COVID-19 associated mucormycosis reveals skull base osteomyelitis in the form of enhancement of left petrous apex (red arrow) (a), pneumatization of sphenoid sinus into pterygoid pates with mucosal thickening of left pterygoid plate (white arrow), with soft tissue in left pterygomaxillary fissure (white arrowhead) (b), along with hypoenhancing soft tissue in the left vidian canal (black arrow) (c). There is also involvement of the left lateral pterygoid muscle (white asterisk) by the disease process with enhancement of the left pterygoid wedge (curved white arrow) at the site of attachment of pterygoid muscles as compared with right side (d). COVID-19, coronavirus disease 2019; MR, magnetic resonance.



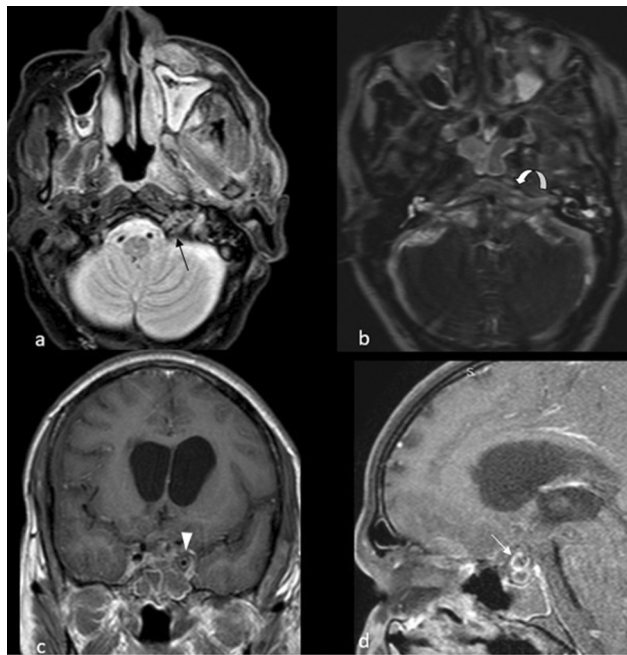


**Fig. 15** Axial short tau inversion recovery (STIR) image (a) of skull base in the same patient as in **–Figs.12 and 13** demonstrates bilateral maxillary sinusitis with extensive inflammation of left pre-antral, prezygomatic soft tissue and left infratemporal fossa. There is abnormal hyperintensity in left jugular fossa as compared with right side, suggesting perineural involvement (*black arrow*). Axial heavily T2W sequence (b) reveals extension of exudates from prepontine cistern to left internal auditory canal, with perineural spread of infection (*curved white arrow*). Coronal T1W postcontrast image (c) shows sphenoid sinusitis and perivascular spread of disease along cavernous segment of left internal carotid artery, causing its luminal narrowing (*white arrowhead*). Postcontrast T1W fat saturated sagittal sequence (d) depicts pituitary involvement as well as a suprasellar peripherally enhancing abscess (*white arrow*).

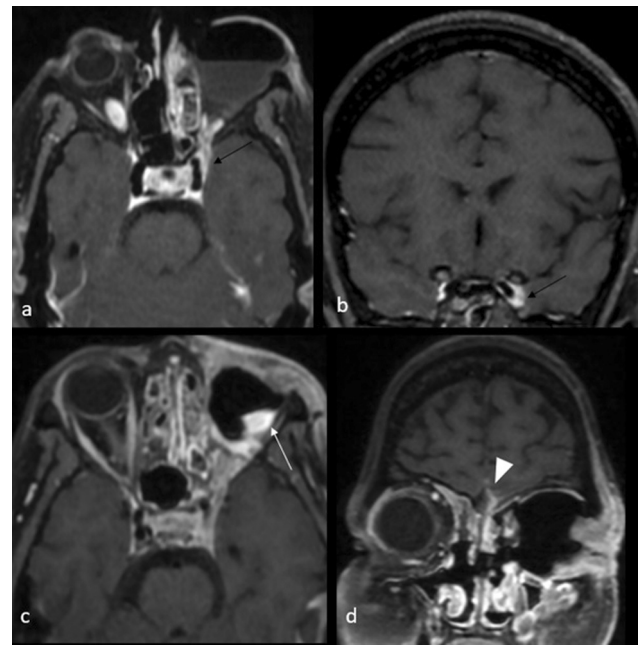


**Fig. 16** Follow-up MRI done in a 38-year-old patient who had undergone treatment with antifungal medication, endoscopic sinus surgery and left sided exenteration for post-COVID-19 rhino-orbital-cerebral mucormycosis reveals residual disease in left orbital apex and cavernous sinus (*black arrow*) as evidenced by enhancing soft tissue on 3-D isotropic T1W fat saturated postcontrast axial (a) and coronal (b) sequences. Note made of residual left ethmoidal sinusitis and air-fluid level in left orbit. Follow-up MRI scan in another 54-year-old female with similar history and management is shown. 3-D isotropic T1W fat saturated postcontrast axial (c) and coronal (d) images demonstrate residual enhancing inflammatory tissue in left orbit (*white arrow*) with extension of disease process into orbital apex, cavernous sinus, and periorbital soft tissue. There is leptomeningeal enhancement in left frontal lobe (*arrowhead*) suggesting residual meningitis. COVID-19, coronavirus disease 2019; MRI, magnetic resonance imaging.

**Table 1** Imaging correlates for various neurological manifestations of COVID-19 associated mucormycosis

Manifestations	Pathophysiology	Imaging correlate
Headache	Involvement of pain sensitive structures in brain like meninges, large pial arteries, venous sinuses, and trigeminal nerve. Extracranial pain may arise from scalp.	Invasive sinusitis extending to superior orbital apex and cavernous sinus, meningitis, venous sinus thrombosis, vasculitis, and trigeminal neuritis.
Proptosis and retroorbital pain	Results from increase in intraorbital content from invasion, extraocular muscle infiltration, or sequelae of vascular or neural involvement.	Retroocular soft tissue, optic neuritis or perineuritis, ophthalmic artery thrombosis/vasculitis, cavernous sinus thrombosis.
Ptosis/diplopia	Occurs from myogenic, neurogenic or mechanical cause	Signal intensity changes and swelling of extraocular muscles, third nerve involvement at the level of superior orbital apex or cavernous sinus
Diminution of vision	Optic nerve involvement	Optic nerve or optic nerve sheath intensity changes with enhancement, or compression of optic nerve by damaged soft tissue in retro-orbital space.
Facial numbness		

**Table 1** (Continued)

Manifestations	Pathophysiology	Imaging correlate
	Trigeminal nerve involvement at cavernous sinus, brain stem, subarachnoid space or at the level of terminal small facial branches involvement.	Trigeminal nerve enhancement with abnormal signal intensity
Facial deviation	Facial nerve involvement, either lower motor neuron (LMN) or upper motor neuron (UMN) type. UMN type palsies are associated with infarction. LMN type facial nerve palsies from peripheral involvement by invasive mucormycosis either at the level of parotid gland or due to vasa nervosum angioinvasion by mucor causing infarction of facial nerve at the level of parotid or when it emerges through the parotid gland.	Brain stem infarction in UMN palsies, Parotid gland signal intensity changes and enhancement, extensive involvement of soft tissue of cheek in LMN palsies.
Bulbar symptoms	Palatal and pharyngeal muscle weakness	Abnormal signal intensity of palatal and pharyngeal muscles with surrounding soft tissue, representing direct invasion of fungus
Stroke	Involvement of cavernous segment of internal carotid artery	Superficial and deep watershed infarcts with or without hemorrhagic transformation
Seizure/disorientation	Brain parenchymal or meningeal involvement most commonly by direct infiltration into frontal and temporal lobes	Cerebritis or brain parenchymal invasion, meningitis.

Abbreviation: COVID-19, coronavirus disease 2019.  
 Source: Adapted from Dubey et al.<sup>3</sup>

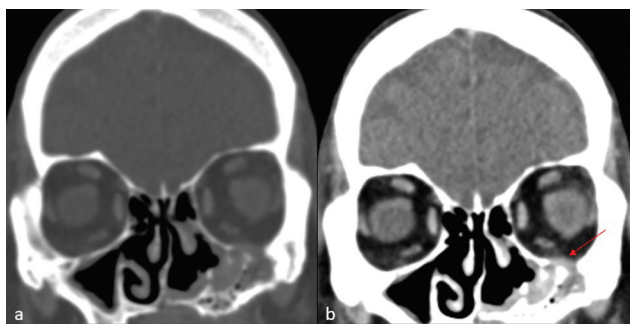


**Fig. 17** Postoperative NCCT scan of paranasal sinuses in a 63-year-old female COVID-19 recovered patient with invasive mucormycosis reveals extensive erosive destruction of all walls of left maxillary sinus on coronal reformatted bone window image (a) with associated residual hyperdense soft tissue extending into the left orbital extraocular fat (red arrow) on soft tissue window (b). Left inferior and middle turbinates are missing suggesting postoperative changes. COVID-19, coronavirus disease 2019; NCCT, noncontrast computed tomography.

**Conflict of Interest**

The authors have no conflicts of interests.

**Acknowledgment**

Department of Radiodiagnosis, Vardhman Mahavir Medical College and Safdarjung Hospital, New Delhi-110029 has been the source of all images used in this manuscript.

**References**

1 Awal S, Biswas S, Awal S. Rhino-orbital mucormycosis in COVID-19 patients—a new threat? *Egypt J Radiol Nucl Med* 2021;52(152)

2 Tooley AA, Bradley EA, Woog JJ. Rhino-orbital-cerebral mucormycosis-another deadly complication of COVID-19 infection. *JAMA Ophthalmol* 2022;140(01):73-74

3 Dubey S, Mukherjee D, Sarkar P, et al. COVID-19 associated rhino-orbital-cerebral mucormycosis: an observational study from Eastern India, with special emphasis on neurological spectrum. *Diabetes Metab Syndr* 2021;15(05):102267

4 Chikley A, Ben-Ami R, Kontoyiannis DP. Mucormycosis of the central nervous system. *J Fungi (Basel)* 2019;5(03):59

5 Gavito-Higuera J, Mullins CB, Ramos-Duran L, Olivas Chacon CI, Hakim N, Palacios E. Fungal infections of the central nervous system: a pictorial review. *J Clin Imaging Sci* 2016; 6:24

6 Saldanha M, Reddy R, Vincent MJ. Title of the Article: Paranasal Mucormycosis in COVID-19 Patient. *Indian J Otolaryngol Head Neck Surg* 2021 (e-pub ahead of print). Doi: 10.1007/s12070-021-02574-0

7 Petrikkos G, Skiada A, Lortholary O, Roilides E, Walsh TJ, Kontoyiannis DP. Epidemiology and clinical manifestations of mucormycosis. *Clin Infect Dis* 2012;54(Suppl 1):S23-S34

8 Maini A, Tomar G, Khanna D, Kini Y, Mehta H, Bhagyasree V. Sino-orbital mucormycosis in a COVID-19 patient: a case report. *Int J Surg Case Rep* 2021;82:105957. Doi: 10.1016/j.ijscr.2021.105957

9 Aribandi M, McCoy VA, Bazan C III. Imaging features of invasive and noninvasive fungal sinusitis: a review. *Radiographics* 2007;27(05):1283-1296. Doi: 10.1148/rg.275065189

10 Galletta K, Alafaci C, D'Alcontres FS, et al. Imaging features of perineural and perivascular spread in rapidly progressive rhino-orbital-cerebral mucormycosis: a case report and brief review of the literature. *Surg Neurol Int* 2021;12:245

11 Lone P, Wani N, Jehangir M. Rhino-orbito-cerebral mucormycosis: magnetic resonance imaging. *Indian J Otol* 2015;21 (03):215

- 12 Sravani T, Uppin SG, Uppin MS, Sundaram C. Rhinocerebral mucormycosis: Pathology revisited with emphasis on perineural spread. *Neurol India* 2014;62(04):383–386
- 13 Taylor A, Vasani K, Wong E, et al. Black turbinate sign: MRI finding in acute invasive fungal sinusitis. *Otolaryngol Case Rep* 2020; 17:100222
- 14 Nguyen VD, Singh AK, Altmeyer WB, Tantiwongkosi B. Demystifying orbital emergencies: a pictorial review. *Radiographics* 2017; 37(03):947–962
- 15 Jain KK, Mittal SK, Kumar S, Gupta RK. Imaging features of central nervous system fungal infections. *Neurol India* 2007;55(03):241–250
- 16 Yang H, Wang C. Looks like tuberculous meningitis, but not: a case of rhinocerebral mucormycosis with Garcin Syndrome. *Front Neurol* 2016;7:181
- 17 Mitra S, Janweja M, Sengupta A. Post-COVID-19 rhino-orbital-cerebral mucormycosis: a new addition to challenges in pandemic control. *Eur Arch Otorhinolaryngol* 2021 (e-pub ahead of print). doi: Doi: 10.1007/s00405-021-07010-1
- 18 Joshi AR, Muthe MM, Patankar SH, Athawale A, Achhapalia Y. CT and MRI findings of invasive mucormycosis in the setting of COVID-19: experience from a single center in India. *AJR Am J Roentgenol* 2021;217(06):1431–1432